

Dimer-vacancy defects on the Si(001)- 2×1 and the Ni-contaminated Si(001)- $2\times n$ surfaces

Ja-Yong Koo, Jae-Yel Yi, Chanyong Hwang, Dal-Hyun Kim, and Sekyung Lee

Korea Research Institute of Standards and Science, P.O. Box 102, Yusong, Taejeon 305-600, Korea

Dong-Hyuk Shin

Department of Physics, Dongguk University, Chung-Gu, Pildong 3-26, Seoul 100-715, Korea

(Received 24 May 1995)

Dimer-vacancy defects on clean Si(001)- 2×1 and Ni-contaminated Si(001)- $2\times n$ surfaces are investigated by scanning tunneling microscopy (STM). The clean Si(001) surface shows the 2×1 reconstruction irrespective of cooling rates faster than $150^\circ\text{C}/\text{sec}$. On the Si(001)- 2×1 surface with a surface dimer-vacancy density of 1.7%, the most abundant dimer-vacancy defect is a randomly distributed one dimer vacancy (1-DV) of the Wang-Arias-Joannopoulos model. Appreciable amounts of (1+2)-DV and 2-DV are observed. The ordered defects on the Si(001)- $2\times n$ surface are mainly composed of (1+2)-DV and 2-DV. The real-space STM images reveal that the dimer adjacent to the unrebonded side of 2-DV is depressed by more than 0.5 \AA , representing the highly asymmetric characteristics. A small amount of Ni contamination on Si(001) drastically increases the dimer-vacancy density from below 2% to above 20%.

I. INTRODUCTION

These days many kinds of electronic devices are fabricated on the Si(001) surface utilizing the low cost and high quality of silicon technology. In the growth of various epitaxial layers on the Si(001) surface, defects play very important roles in determining the qualities of the grown layers. Of defects found on the Si(001) surface, dimer vacancies on the Si(001)- 2×1 structure have been given much attention since the discovery of their abundance by scanning tunneling microscopy (STM).^{1,2} The surface dimer-vacancy density on Si(001)- 2×1 , which ranges from below 1% to 10% or more, is very sensitive to sample preparation processes.^{3,4} Recently the dimer vacancy and dimer-vacancy complexes on the Si(001) surface are studied theoretically based on the experimental results,⁵ explaining the abundance of dimer vacancies and the cluster formation of dimer vacancies.

In a separate branch of studies on the Si(001) surface, either clean or slightly contaminated by Ni or Cu, the existence of the superstructure $2\times n$ has been reported by several groups.⁶⁻¹¹ Martin *et al.*⁷ and Aruga and Murata¹¹ suggested by low-energy electron diffraction that line defects in the $2\times n$ structure should be composed of single missing dimers. Niehus *et al.*⁹ found using STM on the Si(001)- $2\times n$ that several types of dimer-vacancy defects are aligned perpendicular to the dimer rows. They claimed that the dimerization in a third layer below the region of double missing dimers induces the ordered channels. The "split-off" dimer, a complex of a single missing and double missing dimers suggested by them, is similar to the (1+2)-DV (dimer vacancy) of the Wang-Arias-Joannopoulos model.⁵ They have different atomic structures in sublayers. The formation mechanism of the $2\times n$ structure as well as the atomic structure of the complex of dimer vacancies has not been well acknowledged.

In this work we report STM results on the clean Si(001) and the Ni-contaminated Si(001)- $2\times n$. The surface dimer-vacancy density on the clean Si(001)- 2×1 is estimated to be less than 2%. A distribution of complexes of dimer vacancies is somewhat different from that predicted by the theoretical study.⁵ The discrepancy between the models of Niehus *et al.*⁹ and Wang, Arias, and Joannopoulos⁵ on the atomic structure of (1+2)-DV is investigated by applying STM to the Ni-contaminated Si(001)- $2\times n$ and plotting a depth profile over dimer-vacancy defects. The density and distribution of dimer-vacancy defects on the Ni-contaminated Si(001) are evaluated. We compare the natures of dimer-vacancy defects on the clean and the Ni-contaminated Si(001).

II. EXPERIMENTS

The experiments have been carried out in an ultrahigh vacuum below 2×10^{-10} Torr with a scanning tunneling microscope built with a similar structure to the cross-sectional STM of Feenstra *et al.*¹² The electrochemically etched tungsten tip is cleaned *in situ* by electron bombardment. The samples for the clean and the Ni-contaminated Si(001) were cut from a P-doped Si(001) wafer ($10 \Omega\text{cm}$) with the dimension of $10 \text{ mm}\times 4 \text{ mm}\times 0.5 \text{ mm}$. The clean Si(001) samples are prepared carefully so as not to be contaminated by metals. Teflon tweezers are used in handling the samples. The Si(001) samples were wrapped with Ta foil at both ends, mounted on a Mo sample holder without any wet cleaning or etching, and transferred to the STM chamber.

For the Ni-contaminated Si(001), we used stainless-steel tweezers and a stainless-steel sample holder. Other preparation processes are the same as those of the clean Si(001). The small amount of Ni contamination from contacts with the stainless-steel tweezers is sufficient to

stabilize the Si(001)- $2\times n$ structures without any intentional scrubbing of the tweezers against a sample.^{8,9}

After a bakeout of the vacuum chamber, the samples have been outgassed overnight at 700 °C by a direct resistive heating, maintaining the pressure below 2×10^{-9} Torr. After the pressure returns to below 2×10^{-10} Torr, the samples are flashed. During the flashing the pressure is maintained not to exceed 2×10^{-9} Torr. The temperature of the samples is raised slowly by increasing the currents, maintained at 1250 °C for 10 sec, and quenched with initial cooling rates faster than 150 °C/sec. After repeating 20–30 cycles of flashing, clean Si(001) samples show a good 2×1 structure over terraces wider than 2000 Å. By the same process with Ni-contaminated samples we can obtain flat and uniform Si(001)- $2\times n$ with n of 7–8 over the entire sample surface. The heat-treated samples are cooled down for 3 h and transferred to the STM for tunneling images. The calibration of the piezoelectric transducer scanner is performed periodically against 1.36 Å of the layer spacing and 3.84 Å of the surface lattice spacing on the Si(001) surface. The filled state images are obtained with sample bias voltages of –2.0––2.9 V and corresponding tunnel currents of 0.3–0.5 nA.

III. RESULTS

Figure 1 is a typical image of the Si(001)- 2×1 structure quenched from 1250 °C. The numbers of several types of dimer-vacancy defects and a C defect found over 44 500 dimer sites are summarized in Table I. The C defect assumes two successive buckled dimers in the same direction rather than a complex of single atomic vacancies.¹³ The density of the C defect is 0.7% and the total density

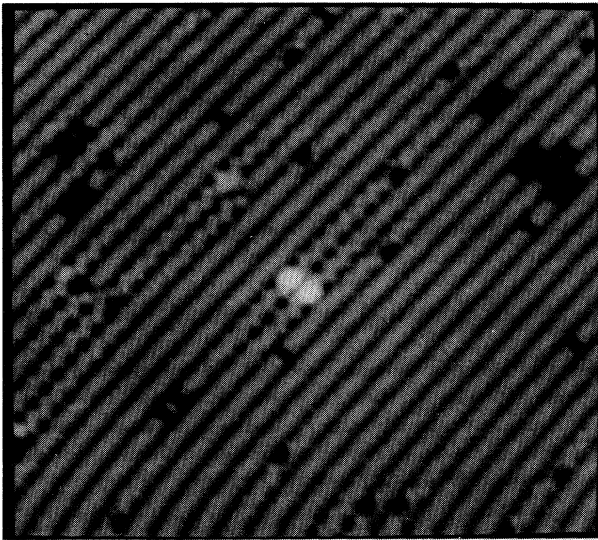


FIG. 1. Typical STM image of the clean Si(001)- 2×1 quenched from 1250 °C with initial cooling rate faster than 150 °C/sec. Sample bias voltage and tunnel current are –2.8 V and 0.3 nA, respectively.

of dimer vacancies is 1.7%. The most dominant dimer-vacancy defect is a single dimer vacancy (1-DV), which is not in agreement with the result by Alerhand *et al.*^{5,14} As pointed out in previous works,^{13,15} the dimer vacancies cause a symmetric effect on neighboring dimers and do not induce any static buckling at room temperature, whereas the effect of the C defect is asymmetric with respect to the dimer row and induces a static buckling of neighboring dimers. As shown in Fig. 1, one C defect buckles more than 20 dimers along the dimer row, implying that 1% of randomly distributed C defects can buckle up to 20% of dimers on a Si(001) surface at room temperature. The cluster of two dimers separated by 1-DV as shown in the center of Fig. 1 induces a strong static buckling along underlying dimer rows. This cluster is a limiting case of small islands with asymmetric step edges. Adjacent buckled dimer rows produce local $c(4\times 2)$ and/or $p(2\times 2)$ structures. All the local patches of $c(4\times 2)$ or $p(2\times 2)$ at room temperature are induced by asymmetric step edges and/or asymmetric defects, not by spontaneous intrinsic dimer interactions. From the buckled dimer rows in Fig. 1, it is found that dimer interactions are strong along the dimer row but are weak in its perpendicular directions. With only a small fraction of asymmetric defects, a considerable fraction of dimers are permanently buckled, screening the intrinsic dimer interactions.

Successive annealing of the quenched Si(001)- 2×1 surface at 700 and 800 °C for 10–20 min does not change appreciably the dimer-vacancy density and the relative abundance of the dimer-vacancy defects. At room temperature any other intrinsic reconstructions rather than 2×1 are not observed on the clean Si(001) quenched with the various cooling rates up to 150 °C/sec or faster.

Figure 2(a) is the image of the Ni-contaminated Si(001)- $2\times n$ structure quenched from 1250 °C. Though the preparation process for Ni-contaminated samples is the same as that for clean samples, results are quite different. As reported by Niehus *et al.*,⁹ the defects are aligned perpendicular to dimer rows, forming straight channels. There are small islands that have been frozen during the quenching. The uniform $2\times n$ structure is also found on those small islands. To see the effect of cooling rates we annealed the quenched sample at 750 °C for 30 min. Figure 2(b) is the resulting image, showing a different aspect from Fig. 2(a). In the annealed sample the line defects are cut frequently, that is, bridged by dimer rows, increasing the length of the average dimer row. Further annealing at 750 °C for 80 min makes the dimer rows longer as shown in Fig. 2(c). A subsequent flashing recovers the structure as shown in Fig. 2(a). A series of flashing and annealing shows a reversible transition between Figs. 2(a) and 2(c).

We compared sizes of various superstructures in quenched and annealed samples. Figure 3 reveals distributions of n values of the Ni-contaminated Si(001)- $2\times n$. The upper histogram is for a sample quenched from 1250 °C and the lower one is for that followed by annealing at 750 °C for 50 min. The annealing results in an appreciable increase of the average value of n . The 2×1 structure is expected with extended annealing.

An enlarged high-resolution STM image shown in Fig.

TABLE I. The numbers of various dimer-vacancy defects and *C* defect on the clean Si(001)-2×1 surface quenched from 1250°C.

Total dimer sites	1-DV	(1+2)-DV	2-DV	(1+1)-DV	(1+3)-DV	(1+1+2)-DV	3-DV	<i>C</i> defect
44 500	316	93	66	7	2	2	2	318

4 well elucidates the atomic structure of the defects on the Si(001)-2×*n*. The majority of defects on 2×*n* are (1+2)-DV and two missing dimers (2-DV), whose occupation exceeds 20% with respect to total dimer sites. The ratio of (1+2)-DV to 2-DV is about 1.5 in the Ni-contaminated sample. In the 2×*n* structure, the fraction

of an isolated 1-DV is relatively small. It appears as a component of dimer-vacancy complexes, for example, (1+2)-DV and (1+2+1)-DV. It is also observed at the end of dimer rows of step edges, as can be seen in Fig. 2(b). Most dimers at the end of dimer rows of the *B* step edge are separated from the dimer row by 1-DV. This

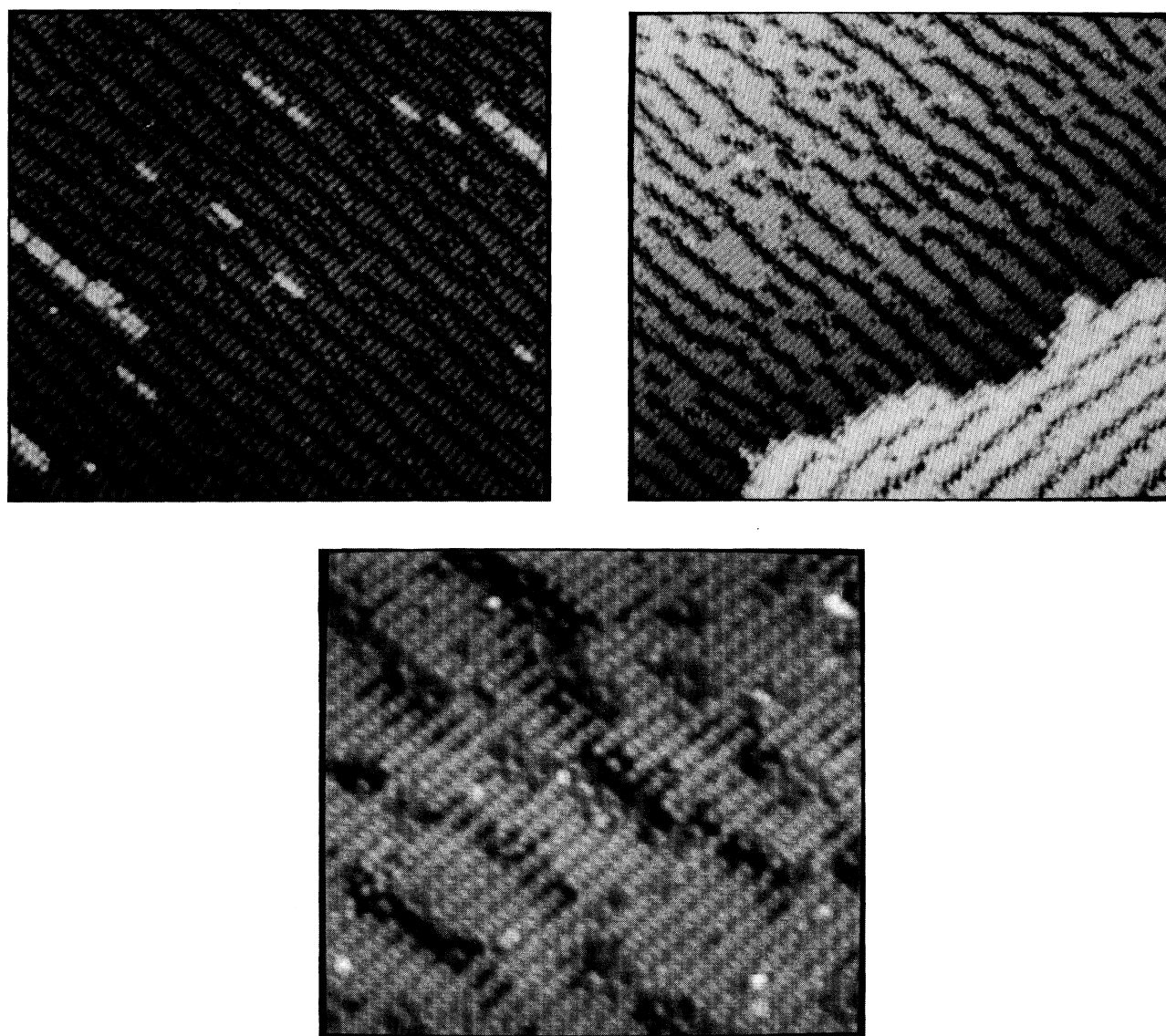


FIG. 2. Ni-contaminated Si(001)-2×*n* prepared by the same process as that for the clean Si(001)-2×1. (b) STM image of the 2×*n* structure annealed at 750°C for 30 min. The average length of the dimer row has increased. At the edge of *B* step most of the dimers are separated from the dimer row by single missing dimers. (c) Further annealed state of the 2×*n* structure. The image has become a 2×1 structure with higher density of defects compared to the clean Si(001)-2×1 (see Fig. 1).

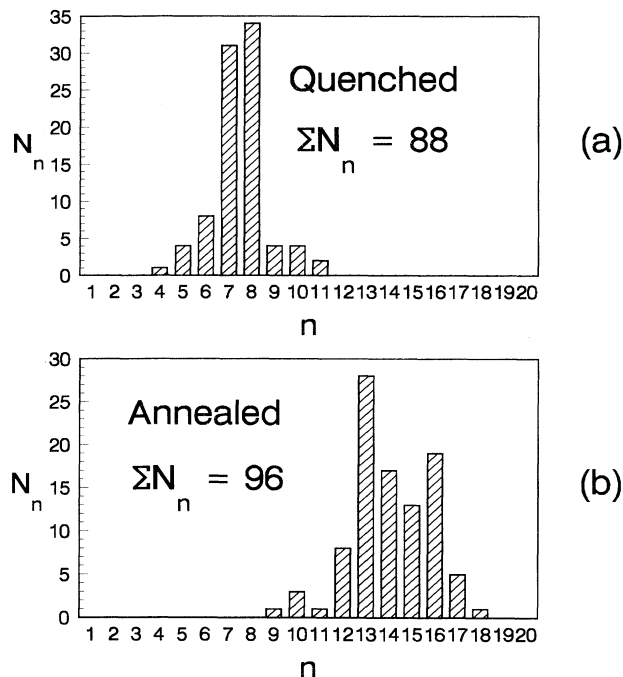


FIG. 3. Distributions of n values for the quenched and annealed $2 \times n$ structures. (a) The superstructure of the quenched $2 \times n$ is approximately 2×7 or 2×8 . The total number of dimer rows considered is 88. (b) The distribution of n values for the sample annealed at 750°C for 50 min. The average length of the dimer row has increased appreciably and the distribution is broader than that for the quenched sample.



FIG. 4. Enlarged STM image of the Ni-contaminated Si(001)- 2×1 structure showing the details of line defects composed of dimer-vacancy defects. One of the two dimers adjacent to 2-DV is depressed and looks gray. The split-off dimer in (1+2)-DV is split into two regions forming a local 1×1 -like structure. Sample bias voltage and tunnel current are -2.3 V and 0.5 nA, respectively.

“split-off” dimer at the step edges is split into two regions forming a local 1×1 -like structure. The C defect is sensitively detected in empty state images and is distributed randomly over dimer rows with the density of 1.2%–1.8%.

The contour plot shown in Fig. 5(a) reveals a depth profile along a dimer row containing (1+2)-DV and 2-DV. The left and right parts are measured over 2-DV and (1+2)-DV, respectively. The contour plot is asymmetric in a region of double missing dimers of (1+2)-DV and 2-DV. Figure 5(b) shows the atomic structure of (1+2)-DV and 2-DV constructed on the basis of the contour plot. Wang, Arias, and Joannopoulos⁵ suggested that the asymmetry of the double missing dimers comes from the rebonding of exposed second-layer atoms. The asymmetric shoulder in (1+2)-DV always appears in the farther side of the double missing dimer region from the split-off dimer. The split-off dimer in (1+2)-DV is also split into two regions forming a local 1×1 -like structure. The asymmetry of 2-DV is apparent, that is, one of the two dimers adjacent to 2-DV is depressed by more than 0.5 Å as shown in Figs. 4 and 5(a). Wang, Arias, and Joannopoulos⁵ pointed out the possible asymmetry of 2-DV in scanning tunneling spectroscopy.

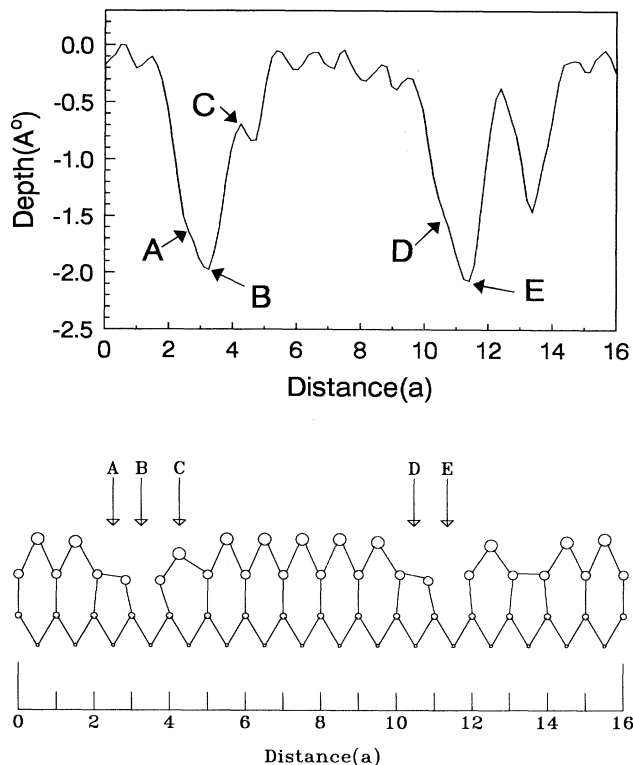


FIG. 5. Depth-profile and atomic model of 2-DV and (1+2)-DV. (a) Contour plot over 2-DV and (1+2)-DV along the dimer row. The region of double missing dimers is asymmetric and the dimer C is depressed into the bulk by more than 0.5 Å. (b) Schematic atomic structure (see text). The unit a in the horizontal axis is 3.84 Å of the surface lattice spacing on the Si(001) surface.

IV. DISCUSSION

The distribution of various dimer-vacancy defects on the Si(001)-2×1 is rather different from that of a previous work done by Wang, Arias, and Joannopoulos⁵ and Alerhand *et al.*¹⁴ The most abundant dimer-vacancy defect is 1-DV in the present result whereas it is (1+2)-DV in the previous one. The major difference between the two results seems to be due to the density of dimer vacancies; 1.7% in the present work and 9% in the previous one. Our samples are quenched from 1250 °C or annealed near 750 °C, representing the freezing-in state of high temperatures above room temperature. A complex of a single dimer vacancy [(1+1)-DV] as shown in Fig. 1, for example, might be an intermediate state transforming to or from 2-DV since vigorous movements of dimer vacancies are expected at high temperatures. With the dimer-vacancy density below 2%, there is less chance for the dimer vacancies to meet and to form dimer-vacancy clusters while the gross uniformity of the dimer-vacancy density over the entire surface is maintained.

Present results show that dimer vacancies on Si(001) tend to form clusters in low concentrations of vacancies even though 1-DV is the dominant defect. Furthermore, the samples with higher dimer-vacancy density by Wang, Arias, and Joannopoulos⁵ and Alerhand *et al.*¹⁴ show the (1+2)-DV as the dominant defect. Therefore, there is a tendency of dimer vacancies to cluster rather than to repel each other when the density of dimer vacancy is high. Many of the long dimer rows on our clean Si(001) do not need missing dimers to reduce dangling bonds by π bonding or to relieve the possible compressive stress. This disagrees with predictions by Pandey.¹⁶

In our experiments the source of Ni contamination is from the contacts of the sample with stainless steel when handling the sample with stainless steel tweezers. Main contaminants from stainless steel would be Fe, Cr, and Ni. Kato *et al.*⁸ pointed out that heavy metals like Fe and Cr could be easily removed by surface evaporation during repeated flashings but Ni could not be eliminated due to its high diffusion coefficients in Si. As to the atomic structures of defects on the Si(001)-2× n , several models have been suggested. Pandey¹⁶ suggested the possibility of the 2× n structure on the clean Si(001) surface in terms of the π -bonded defect. In Pandey's model the dominant defect is the rebonded missing dimer (1-DV), which can be aligned either along or perpendicular to the dimer rows, leading to ordered structures. This model is excluded since our clean sample reveals no superstructure and the dominant defects in the 2× n structure are complexes of dimer vacancies. Martin *et al.*⁷ and Aruga and Murata¹¹ investigated the 2× n structure by low-energy electron diffraction and claimed the dominant defect to be 1-DV, contradicting the present result. On the contrary Niehus *et al.*⁹ found by STM that the dominant defect is (1+2)-DV. They claimed that the defects should be ordered to channels by third-layer dimerization on the basis of the observation that the defect region of double missing dimers is deeper than 1.36 Å of the layer spacing.

The present high-resolution contour plot over the defect region of double missing dimers shown in Fig. 5(a) represents the depth of about 2.0 Å, but it corresponds to the unbonded region *B* and *E* between second-layer atoms as shown in Fig. 5(b) rather than the top of third-layer atoms. The contour plot over the dimer row containing (1+2)-DV and 2-DV agrees well with the Wang-Arias-Joannopoulos schematic model as shown in Fig. 5(b).

Several works have discussed the role of the Ni impurities on Si(001)-2× n .^{8,9,11} Though the underlying mechanism forming the 2× n structure is not clear, only a small fraction of Ni contamination less than 1% is sufficient to stabilize Si(001)-2× n .^{8,9} The most drastic change induced by Ni contamination on Si(001) is the increase of dimer-vacancy density from below 2% to above 20%.

Zandvliet, Elswijk, and van Loenen¹⁷ showed that the excess dimer vacancies created by ion bombardment on clean Si(001) align perpendicular to the dimer rows by moderate annealing. Similar tendencies are found in the experiments of etching of the Si(001) surface by reactive gases followed by annealing.^{18–22} These results represent the intrinsic interaction of dimer vacancies on the Si(001) surface to align perpendicular to the dimer rows when the density of dimer vacancy is sufficiently high. Our STM images on the Si(001)-2× n , apart from the step edges, show that the dominant dimer-vacancy defects are (1+2)-DV and 2-DV with relative populations of 3 to 2. This reflects similar relative formation energies on both the clean and the Ni-contaminated Si(001). Considering the formation of line defects from excess dimer-vacancy defects by annealing^{17–22} and our observations on Si(001)-2× n , we suggest that the Ni impurity on a Si(001) surface simply increases the density of the dimer vacancy drastically by changing the atomic and electronic structures. The next steps of the formation of the 2× n structure are automatically carried out by the intrinsic interaction of dimer vacancies. They tend to form clusters like (1+2)-DV and 2-DV and to align perpendicular to the dimer rows.

V. CONCLUSIONS

The clean Si(001) surface always shows only the 2×1 reconstruction at room temperature regardless of cooling rates up to 150 °C/sec, whereas the Ni-contaminated Si(001) surface shows 2× n structure with varying n in accordance with annealing temperatures and cooling rates. All the local patches of $c(4\times 2)$ and $p(2\times 2)$ on the clean Si(001) at room temperature are induced by asymmetric step edges and/or asymmetric defects, rather than by spontaneous intrinsic dimer interactions. A small amount of Ni contamination on Si(001) increases the density of surface dimer vacancies drastically and stabilizes 2× n structure, where main dimer vacancy defects are (1+2)-DV and 2-DV aligned perpendicular to the dimer rows. The 2× n structure is formed via interactions of dimer vacancies at high density.

ACKNOWLEDGMENTS

One of the authors (J.-Y. Koo) thanks Young Joo Lee for the recipe of radiation quenching in cleaning the Si(001) surface and Dr. R. M. Feenstra for the concepts

of scanning tunneling spectroscopy. This work was supported in part by the Ministry of Science and Technology of Korea, and by the Korea Science and Engineering Foundation through the Science Research Center of Excellence Program.

-
- ¹R. M. Tromp, R. J. Hamers, and J. E. Demuth, *Phys. Rev. Lett.* **55**, 1303 (1985).
- ²R. J. Hamers, R. M. Tromp, and J. E. Demuth, *Phys. Rev. B* **34**, 5343 (1986).
- ³R. J. Hamers, U. K. Kohler, and J. E. Demuth, *J. Vac. Sci. Technol. A* **8**, 195 (1990).
- ⁴N. Kitamura, M. G. Lagally, and M. B. Webb, *Phys. Rev. Lett.* **71**, 2082 (1993).
- ⁵J. Wang, T. A. Arias, and J. D. Joannopoulos, *Phys. Rev. B* **47**, 10497 (1993).
- ⁶E. G. McRae, R. A. Malic, and D. A. Kapilow, *Rev. Sci. Instrum.* **56**, 2077 (1985).
- ⁷J. A. Martin, D. E. Savage, W. Moritz, and M. G. Lagally, *Phys. Rev. Lett.* **56**, 1936 (1986).
- ⁸K. Kato, T. Ide, S. Miura, A. Tamura, and T. Ichinokawa, *Surf. Sci.* **194**, L87 (1988).
- ⁹H. Niehus, U. K. Kohler, M. Copel, and J. E. Demuth, *J. Microsc.* **152**, 735 (1988).
- ¹⁰Y. J. Lee, S. Kim, C.-S. Hwang, C. Lee, and C. Hwang, *Phys. Rev. B* **50**, 11204 (1994).
- ¹¹T. Aruga and Y. Murata, *Phys. Rev. B* **34**, 5654 (1986).
- ¹²R. M. Feenstra, E. T. Yu, J. M. Woodall, P. D. Kirchner, C. L. Lin, and G. D. Pettit, *Appl. Phys. Lett.* **61**, 795 (1992).
- ¹³R. J. Hamers and U. K. Kohler, *J. Vac. Sci. Technol. A* **7**, 2854 (1989).
- ¹⁴O. L. Alerhand, N. A. Berker, J. D. Joannopoulos, D. Vanderbilt, R. J. Hamers, and J. E. Demuth, *Phys. Rev. Lett.* **64**, 2406 (1990).
- ¹⁵R. A. Wolkow, *Phys. Rev. Lett.* **68**, 2636 (1992).
- ¹⁶K. C. Pandey, in *Proceedings of the Seventeenth International Conference on the Physics of Semiconductors*, edited by D. J. Chadi and W. A. Harrison (Springer-Verlag, New York, 1985), p. 55.
- ¹⁷H. J. W. Zandvliet, H. B. Elswijk, and E. J. van Loenen, *Phys. Rev. B* **46**, 7581 (1992).
- ¹⁸D. Rioux, M. Chander, Y. Z. Li, and J. H. Weaver, *Phys. Rev. B* **49**, 11071 (1994).
- ¹⁹K. Wurm, R. Kliese, Y. Hong, B. Rottger, Y. Wei, H. Neddermeyer, and I. S. T. Tsong, *Phys. Rev. B* **50**, 1567 (1994).
- ²⁰D. Rioux, R. J. Pechman, M. Chander, and J. H. Weaver, *Phys. Rev. B* **50**, 4430 (1994).
- ²¹D. Rioux, F. Stepniak, R. J. Pechman, and J. H. Weaver, *Phys. Rev. B* **51**, 10981 (1995).
- ²²Y. Wei, L. Li, and I. S. T. Tsong, *Appl. Phys. Lett.* **66**, 1818 (1995).

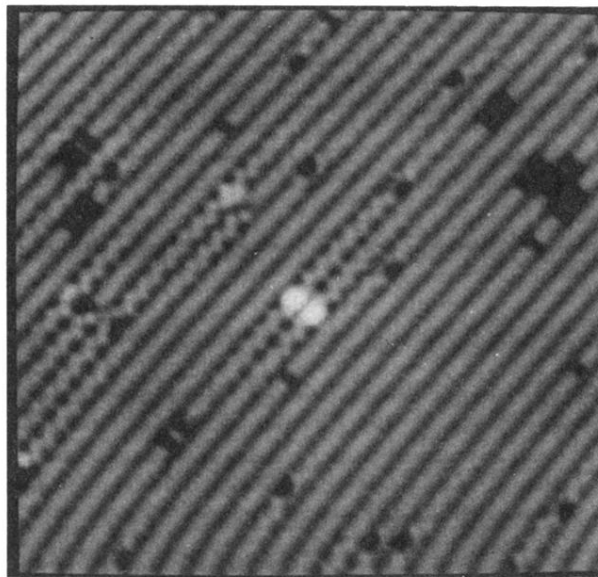


FIG. 1. Typical STM image of the clean Si(001)-2 \times 1 quenched from 1250°C with initial cooling rate faster than 150°C/sec. Sample bias voltage and tunnel current are -2.8 V and 0.3 nA, respectively.

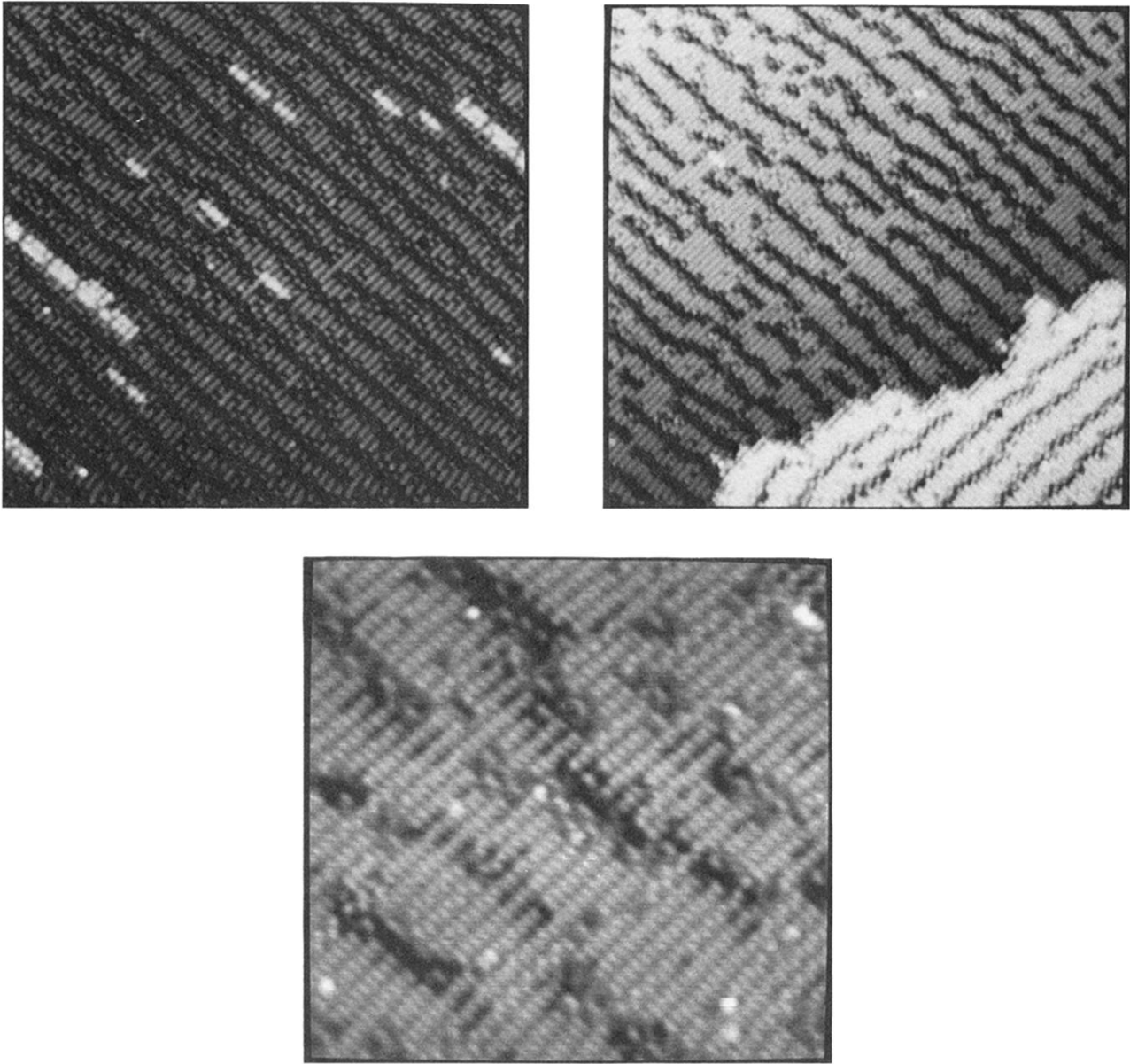


FIG. 2. Ni-contaminated Si(001)- $2\times n$ prepared by the same process as that for the clean Si(001)- 2×1 . (b) STM image of the $2\times n$ structure annealed at 750 °C for 30 min. The average length of the dimer row has increased. At the edge of B step most of the dimers are separated from the dimer row by single missing dimers. (c) Further annealed state of the $2\times n$ structure. The image has become a 2×1 structure with higher density of defects compared to the clean Si(001)- 2×1 (see Fig. 1).

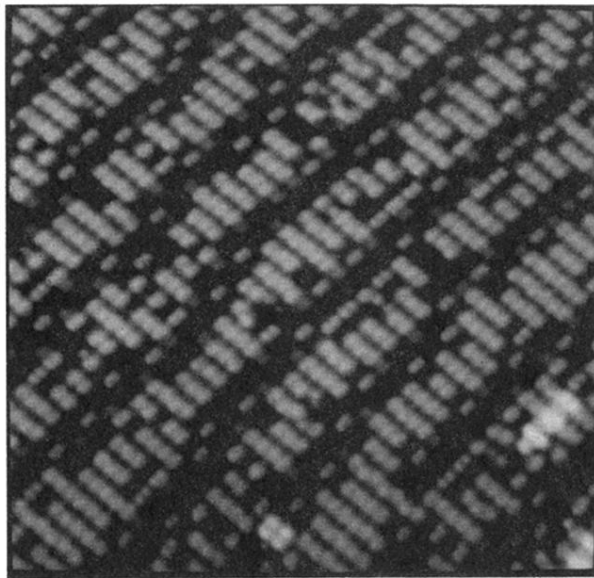


FIG. 4. Enlarged STM image of the Ni-contaminated Si(001)- 2×1 structure showing the details of line defects composed of dimer-vacancy defects. One of the two dimers adjacent to 2-DV is depressed and looks gray. The split-off dimer in (1+2)-DV is split into two regions forming a local 1×1 -like structure. Sample bias voltage and tunnel current are -2.3 V and 0.5 nA, respectively.